ISSN 0252-1075
Research Report No. RR-082

Contributions from
Indian Institute of Tropical Meteorology

EVALUTION OF CONVECTIVE BOUNDARY LAYER OVER THE DECCAN PLATEAU DURING SUMMER MONSOON

by

S. S. PARASNIS

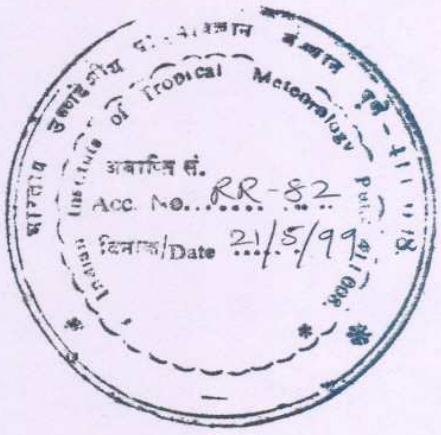

PUNE - 411 008
INDIA

FEBRUARY 1999

CONTENTS

EVOLUTION OF CONVECTIVE BOUNDARY LAYER OVER THE DECCAN PLATEAU DURING SUMMER MONSOON

Surendra S. Parasnis

Indian Institute of Tropical Meteorology, Pune

Abstract

Characteristic features of the convective boundary layer (CBL) have been explored using the saturation point analysis and conserved variable approach. The aerological observations (between 1130 - 1230 LST) over Pune (18°32' N, 73° 51'E, 559 m AMSL) during two summer monsoon seasons (1980, 1981) have been used for this purpose. The results of the investigations indicated that (i) the top of the CBL varied between 700-600 hPa during different activities of the summer monsoon. (ii) the air above the top of the CBL during week monsoon activity appeared to subside at the rate of 30 hPa per day.

1 Introduction

The convective boundary layer, mostly the daytime boundary layer, is defined as the region where there is a upward heat flux. In the afternoon there might exist a relatively deep (1-3 km) convective mixed layer, so called because turbulence is so intense that momentum, heat ,moisture and tracers are mixed relatively uniformly with height by convective processes. At the top of this mixed layer there is a statically stable layer call entrainment zone, across which the variables listed above change from their boundary layer value to free atmosphere value. Clouds might be present if sufficient moisture is present in the boundary layer. In CBL, the turbulence in the mixed layer entrains less turbulent air from above. The entrainment processes cause the mixed layer to grow in thickness in time by mixing into it air with properties (momentum, temperature and humidity and traces) characteristics of free atmosphere. Over land, the convective boundary layer (CBL) plays an important role in regulating the transport of energy and moisture upward into the atmosphere from earth's surface.

The thermodynamic structure of the CBL over oceanic regions was well investigated from 'conserved variable analysis' (Betts and Albrecht, 1987). The diagnostic studies of CBL could be useful to guide the development of mixing line boundary layer cloud parameterisation that has been proved to be important in global climate models (Betts, 1986; Betts and Miller, 1986).

Betts in early eighties (1982) introduced the Saturation Point (SP) representation of moist thermodynamics, showing how the approach is useful in understanding the cloud processes in terms of conserved thermodynamic variables. If the cloud topped boundary layer has distinct source region of constant SP such as ocean surface or the dry inversion air above its top, the state of the atmosphere in between can be conveniently expressed in terms of linear variations along a mixing line of the conserved SP properties. Deviations from this mixing line are then caused by radiation, and precipitation (Boers and Betts, 1988).

When a parcel of unsaturated air is lifted adiabaticaly to a level where it gets saturated with the available moisture that level is called as the lifting condensation level (LCL). Betts (1982) called this level as saturation level and a point on it a Saturation Point (SP). The SP can be obtained using the T and Td observations at any particular level. Since the SP remains unchanged during adiabatic ascent or descent, it can be used as thermodynamic tracer of an air parcel. The SP can be specified uniquely by θ, θ_e and q at saturation level. The difference between

the data pressure level and pressure at saturation level (P_{SL}), which plays an important role in the mixing processes, is defined as

$$P^{*} = P_{SL} - p$$

Thus P^{*} is the saturation pressure deficit (Betts, 1982). The SP of the mixture of two air parcels at different levels can be obtained easily by taking the average of the thermodynamic parameters such as potential temperature (θ) mixing ratio (q) associated with the saturation points of two air parcels at different levels. The line joining the SP's of all mixtures is the mixing line. The conserved variable diagrams (θ_e - q) depict characteristics mixing line from surface to the top of the CBL. The top of the CBL appears as a marked change in slope of q or reversal of q in these diagrams.

In this study, the same analysis has been used to study the thermodynamic structure of the CBL during the summer monsoon over the Deccan Plateau region of India.

The large - scale circulation, inherent in the monsoon flow, seems to affect the motions of the order of a few kilometers, essentially a boundary-layer-type of scale (Holt and Sethuraman, 1986). In this study, the aerological observations carried out during two consecutive summer monsoon seasons viz. 1980 and 1981, have been used to study the thermodynamic structure of the CBL. The observations have been grouped into different categories depending on the areal rainfall and synoptic weather conditions. The purpose of this study is to show how the CBL thermodynamic structure over land region during summer monsoon season can be expressed in terms of distribution of SP parameters.

In Section 2 location of observations and the meteorological conditions are presented. The method of analysis of the observations has been given in section 3. Section 4 deals with the results obtained related to average CBL structures during summer monsoon seasons of 1980 and 1981. The CBL structures during the different categories (based on areal rainfall) are presented. The characteristic CBL structures during the two periods of contrasting synoptic weather conditions are also discussed. Conclusions and scope for future study are given in Section 5.

2 Location of observations and meteorological conditions

Pune (18^{0} 32'N, 73^{0} 51'E, 559 m ASL), is situated in the Deccan Plateau region (Figure 1), and is not a routine aerological station. However, special aerological observations were carried out during the summer monsoon seasons of 1980- 1981, in connection

with the artificial rain-making experiment conducted by the Indian Institute of Tropical Meteorology. The observational period was from the last week of June to first week of September. There were a total of 162 days' observations taken between 1130- 1200 UTC. Synoptic situations which are more favourable for prominent weather development over this region are i) southerly positioned monsoon trough, ii) monsoon depression and cyclonic circulation, iii) Mid-tropospheric circulation (MTC) positioned in the vicinity of the region, iv) cyclonic storms and pre -and post-monsoon thunderstorm activities. (Parasnis, 1991).

3 Method of analysis

3.1 Categorization of observations

The aerological observations during the summer monsoon seasons of 1980 and 1981 were classified into four different categories, according to the rainfall activity over the Madhya Maharashtra area, as Pune is a representative of the area. The information of daily rainfall activity reported as widespread (W), fairly widespread (FW), scattered (Sc) and isolated (Iso) was obtained from the publications of India meteorological Department. These classification correspond to > 75%, 51-75%, 26-50% and 1-25% respectively of this area. The aerological observations were first averaged at every 50 hPa level interval, T and Td were then obtained at each 10 hPa interval by a simple linear interpolation which were then used to compute the thermodynamic parameters at 10 hPa intervals extending from the surface to 500 hPa. The average values of T and Td in the respective categories at an interval of 10 hPa were used to compute the thermodynamic parameters such as potential temperature (θ,), virtual potential temperature (θ_v), equivalent potential temperature (θ_e), saturation equivalent potential temperature (θ_{es}), mixing ratio (q), and saturation level pressure (P_{SL}).

Further, two periods of 6 days duration were selected on the basis of synoptic weather conditions. During the two periods the synoptic weather conditions were contrasting to each other. The CBL structures during the two periods were used to compare with those obtained in the above four categories.

3.2 Conserved variable diagram

A schematic conserved variable diagram (Figure 2) is reproduced from Betts and Albrecht (1987) which shows a mixing line between the SP's of the mixed layer and the CBL top on a (θ_e, q_T) diagram. The axes represent conserved variables in the absence of irreversible diabatic processes. The condensation process does not change θ_e or q_T but the precipitation process moves to lower q

and the evaporation of falling precipitation moves to higher q at constant θ_e. The radiative cooling moves to lower θe at constant q. Mixing lines are straight lines on this diagram and advective processes do not move parcel points at all. The thermodynamic changes are shown in Figure 2 by a triangular path. The situation in tropical circulation is such that the precipitation in the descending deep convection branch moves parcels from the sub-cloud layer to lower q at constant θ_e and radiative cooling in the subsiding branch lowers θ_e at constant q. The air in the lowest θ_e sinks into the CBL and its SP moves down the mixing line as it is mixed with air from below, on its final mean descent back into the sub-cloud layer.

4 Results and discussion

4.1 Average CBL structure

Figures 3a shows the plots of q, θ_v, θ_e, and θ_{es} averaged at 10 hPa against pressure from 950 hPa (surface) to 500 hPa and Figure 3b shows the plot of P_{SL} and $P^* = (P_{SL}-P)$ for the summer monsoon of 1980. Similarly Figures 4a and 4b show for the year 1981. Negative values of P^* are related to the layer subsaturation. The typical three layer structure (sub-cloud, cloud and capping layer) of the CBL is quite apparent from these Figures. The sub-cloud layer has almost constant θ_v from 900-850 hPa (Figures 3a and 4a). There is a distinct moist layer (cloud layer) from 850-750 hPa which is unstable in θ_{es} at the base and has a nearly constant value of P^* (-40 hPa). The cloud layer is capped by a stable layer. The top of the stable layer (also CBL top) is marked by minimum of θ_e (650 hPa). The minimum value of P^* at the top of the stable layer is a distinguished characteristic feature observed in these average CBL structures (Figures 3b and 4b). Another characteristic feature of the average observations is that of a constant P^* layer above the top of the CBL. This layer with P^* values of -80 hPa seen from 650-600 hPa, indicates very dry air conditions at the top of the CBL. It will be of interest to find the origin of such dry air. During the monsoon of 1980, the P^* plot shows a reversal of gradient in the layer below sub-cloud layer. This may be due to the subsaturation at 900 hPa which is higher than that at the surface.

4.2 CBL structure during different categories

The observations in the two summer monsoon seasons (1980 and 1981) have been divided into four different categories of rainfall. The CBL structures, evaluated under each category are presented below.

4.2.1 Isolated rainfall category (Iso)

Figure 5a shows the averages of q, θ_v, θ_e, θ_{es} from surface up to 500 hPa under isolated rainfall (1-25 %) category. They are

representations of average of 39 soundings. The sub-cloud layer from 900-830 hPa nearly follows constant θ_v. There is moist adiabatic layer from 830-750 hPa, which is capped by a stable layer (750-700 hPa). The stable layer is marked by θ_{es} maximum. Indeed, there was an inversion layer between 750- 700 hPa (which will be discussed in Section 4.4), on nearly 6 days. The θe minimum is not found at CBL top (700 hPa) but at 650 hPa. It is also seen that the mean sub-cloud θ_e of 353 K exceeds the θ_{es} maximum at 700 hPa of 347 K. This indicates that there may have been intermittent convection in this category which has penetrated the inversion layer. This was also noticed in BOMEX observation (22-24 June, 1969) where the θ_e minimum was observed 150 hPa above the top of the CBL (Betts and Albrecht, 1987).

Figure 5b shows a plot of P* and P_{SL} under this rainfall category. The cloud layer is marked by constant P* value of -43 hPa (830-750 hPa), which reflects rather dry cloud layer. Above the cloud layer, there is a sharp decrease of P* up to the top of the stable layer at 700 hPa. The minimum value of P* occurred at 700 hP corresponds to maximum of θ_{es} at that level. From 700-650 hPa P* remained constant and above 650 hPa, it shows a gradual increase (-98 hPa).

4.2.2 Scattered rainfall category (Sc)

The averages of q, θ_v, θ_e, θ_{es} under this rainfall category (26-50 %) are shown in Figure 6a. It is a representation of average of 61 soundings. The surface layer shows unstable stratification similar to the aforesaid isolated rainfall category. The sub-cloud layer (900-840 hPa); the cloud layer (up to 750 hPa) and the capping stable layer (750-650 hPa) depict characteristic gradients of q, θ_e, and θ_{es}. θ_e minimum is at 650 hPa which marks the top of the CBL. The averages of P* and P_{SL} under this category are shown in Figure 6b. There are only few differences in the profiles under the two categories (Iso and Sc). The P* minimum value is seen at 650 hPa. Both θe and P* show minimum values at the top of CBL in this category. The cloud layer (840-750 hPa) has constant value of P* (-42 hPa). The sharp decrease of P* in the capping stable layer, observed in isolated rainfall category is not observed here. The reason for this is the strong capping stable layer (750-700 hPa) observed in isolated rainfall category has been weakened with the increase of CBL depth.

4.2.3 Fairly widespread rainfall category (Fw)

In the earlier two categories the monsoon activity was weak. This category represents enhancement of monsoon activity as seen from the rainfall distribution in this category i.e. 51-75%. Figure 7a shows the q, θ_v, θ_e, θ_{es} averages under this category. It is a representation of average of 48 soundings. The features are similar

to those of earlier two categories except that θes shows slightly neutral stability in the cloud layer though it is unstable at the cloud base. Figure 7b shows P* and P_{SL} plots under this category. P* minimum is at 630 hPa which coincides with turning point towards decreasing θ_e and increasing θ_{es}. The P* average shows constant values (-36 hPa) which corresponds to 82% relative humidity from cloud base (850 hPa) to cloud top (750 hPa). The reversal of P* in the layer below sub-cloud layer as observed in the previous categories is seen less marked here.

4.2.4 Widespread rainfall category (W)

Figure 8a shows q, θ_v, θ_e, θ_{es} averages under this category. It is a representation of the average of 14 soundings. This category represents moderately active monsoon conditions as seen from the rainfall coverage (more than 75% of the area). θ_e average shows almost constant minimum value from 650-600 hPa. The minimum value of P* (Figure 8b) is seen at 600 hPa. The CBL top in this category is taken as 600 hPa. θ_{es} averages show almost constant value (345 K) from 800 hPa above. The distribution of q in Figure 8a shows two layers from surface to 900 hPa and 900 hPa aloft. The P* average shows constant value of -23 hPa (which corresponds to 88% relative humidity) from 860-750 hPa which indicates the cloud layer. There is another layer of constant P* from 600- 500 hPa (P*= -40 hPa) above the CBL top, suggesting a possibility of another cloud layer. In an earlier study (Selvam et. al.,1982), using the aerological observations at Pune, it was noticed that during the active monsoon period, in the vertical distribution of relative humidity, there were two peaks, one in the region 850-750 hPa and another in the region of 600-500 hPa. This indicated the existence of two cloud layers.

In the discussion of CBL structure above, the θ_{es} maximum was found very much marked only in the isolated rainfall category. Capping stable layer between 750-700 hPa was quite strong in this category. In general, in other three categories θ_{es} remained almost constant from 800 hPa above. The most important parameter to determine CBL top is P*. In all the above categories, the CBL top and cloud layer are determined mostly by P* which is an important parameter in determining the CBL top and put by (Betts and Albrecht, 1987)

4.3 Conserved variable diagrams under various rainfall categories

The conserved variable diagrams (θ_e-q) for the aforesaid four categories are shown in Figures 9(a-d). The pressure levels are also marked in these diagrams. Intervals of 50 hPa are shown by solid circles and joined by broken lines. These broken lines in fact represent the mixing lines. A mixing line (ML) is produced when the vertical convective mixing dominates over the processes that do not

conserve air parcel SP, such as radiative cooling or the processes of precipitation and evaporation of falling rain. The precipitation-evaporation couplet, which closely conserves θ_e, does not produce either a θ_e or q reversal between the two layers. It could split a single mixing line into two with a step in q because the precipitation (evaporation) process moves SPs at the constant θ_e to lower (higher) q. Radiative uncoupling that conserves q, but not θ_e, could produce a θ_e reversal between two layers (Betts and Albrecht, 1987).

Here all these diagrams show a single ML structure from surface to CBL top. In the Isolated rainfall category the CBL top is 700 hPa. There is a change in slope above 700 hPa as shown in Figure 9a. Also, the strong stable layer between 750-700 hPa is marked by larger gap between these two points. The sub-cloud layer in all the categories between 900-850 hPa, follows a constant θ_v isopleth. For Scattered rainfall and Fairly widespread rainfall categories (Figures 9b and 9c) the cloud layer and the capping stable layer show change in ML slope. In Figure 9d, the cloud layer and capping stable layer, are represented by a single mixing line, for Widespread rainfall category. In general, the mixing line structures in all the categories, from surface to the top of the CBL, could be represented by single mixing line in these diagrams.

A distinct picture of the CBL structures emerges from these diagrams (Figures 9a-9d). The CBL has shown characteristic ML structure up through cloud and capping stable layers to the top of the CBL. The layer from surface to CBL top is thermodynamically coupled to the surface. The air above the CBL is not coupled thermodynamically to the surface and is usually sinking with radiative cooling. The top of the ML is characterized by θ_e minimum and P^* minimum. The air just above the CBL as it cools sinks, reaches minimum θ_e before entering the CBL.

4.4 Characteristic CBL structures during active and break monsoon conditions

The CBL structures discussed in the earlier Section represent the CBL during different activities of monsoon, based on areal averaged rainfall. In this Section, the characteristic changes in CBL structure associated with contrasting weather conditions in the summer monsoon of 1980 are brought out. For this purpose ,a 6 day's active monsoon period (August) and a 6-day 'break monsoon' period (July) are chosen.

4.4.1 Synoptic weather conditions

The two periods of contrasting synoptic weather conditions are chosen on the basis of the positions of monsoon trough. During

1-6 August ,1980 the monsoon trough is situated along the Gangetic Plains protruding into the Bay of Bengal, thus comprises of an active monsoon period. (Rao, 1976). Similarly, during 12-17 July 1980, the monsoon trough migrated farther to the north and lay along the foot-hills of the Himalayas, thus comprises a 'break monsoon' period.(Sikka, 1978). The synoptic weather charts on 13 July and 3 August are shown in Figures 10, showing the break and active monsoon conditions respectively. The period of active monsoon conditions (1-6 August) is also characterised by a cyclonic circulation existing in the lower troposphere over the central parts of India .

4.4.2 CBL structure during active and break monsoon periods

Figures 11a and 12a show the profiles q, θ_v, θ_e and θ_{es} (averages) during the break and active monsoon periods. The P* and P_{SL} (averages) plots during the respective periods are shown in Figures 11b and 12b. Interestingly, an inversion layer is observed between 750-700 hPa during break monsoon period. θ_v averages show increase in stability between 750-700 hPa. This inversion layer was also observed on each individual day. The moist adiabat through θ_e at 930 hPa (representing the temperature path of an ascending nonentraining air parcel) showed positive buoyancy above the LCL of 930 hPa air, but again intersected the θ_{es} sounding below 500 hPa. θ_e curve shows change in the conditional instability, highly unstable between 750 and 700 hPa above which it is ceased. From profile, it is evident that there exists high instability in the surface layer during break monsoon period. The base and top of the inversion layer are marked by θ_{es} minimum and maximum respectively. From Figure 11b, it can be noticed that the top of the inversion layer is associated with P* minimum. Thus, during the break monsoon period the CBL top is at 700 hPa and is in association with P* and θ_e minima and θ_{es} maximum. Also seen is a cloud layer between 850-750 hPa with a constant subsaturation (P* = -40). The P_{SL} averages show different gradients in sub-cloud, cloud and inversion layers.

θ_e averages during the two periods of contrasting weather conditions show differences. In the layer between 900-800 hPa the instability is more in the case of active monsoon period as compared to that in break monsoon period. During active period it shows almost same gradient in the layer 900 hPa above (Figure 12b). The averages during the active monsoon period show cloud layer from 870 hPa above. A characteristic distribution of P* is seen in Figure 12b. The increase in P* above 700 hPa indicates another cloud layer.

4.4.3 Origin of the CBL top air

The CBL top is marked by minimum of P* values. P* is very useful parameter to distinguish between layers that are in and above CBL. In absence of radiation and mixing processes, the

saturation level of a parcel (PSL) is unchanged by vertical (dry or moist adiabatic) motion, so that if air above the CBL subsides faster than the radiative excess of P_{SL}, then P* can reach relatively large negative values. At the top of the CBL, no layer of constant P_{SL} values is observed in the present study unlike observed over the Pacific Oceanic regions (Betts and Albrecht, 1987). But a layer of dry air (P* -75 to -100 hPa) is observed above the top of the CBL. The origin of the CBL top air can be estimated by using conservation of q, provided the vertical structure of q of the atmosphere is known where this air is originated. The CBL tops in the four categories have been indentified as 700, 650,630 and 600 hPa. During the break monsoon period the CBL top was at 700 hPa like that in isolated rain category. Determination of CBL top is based on minimum values of P* and θ_e. In the presence of an inversion layer, maximum value of θ_{es} was also found at the CBL top.

In Table 1, the SP parameters are given at the CBL top for the isolated rainfall category and break monsoon period in the upper panel and for widespread rainfall category and active monsoon period in the lower panel also given where the averages cross the q values corresponding to CBL top air in the isolated rainfall category and break monsoon period. The differences in the values indicate that the CBE top air has subsided 100 and 180 hPa respectively in the two cases, while cooling of the order 6.3 and 10 K respectively was associated with this subsiding air.

If the radiative cooling rate is assumed as -1.75 K day^{-1}, it corresponds to 4-6 days of subsidence at 28-32 hPa day^{-1}. It is clear that the air at the CBL top has subsided from a level just above the freezing level. It is interesting to see the modification of P^* during descent. As the parcel sinks with radiative cooling, its P^* and P_{SL} change.

$$\bar{P} = \bar{P}_{SLR} - \bar{p} = \bar{P}_{SLR} - \omega$$

here $\omega = \partial p / \partial t$.

The radiative cooling of saturation level is given by

$$\bar{P}_{SLR} = -\frac{\bar{\theta}_R}{\left(\frac{\partial \theta}{\partial p_{SL}}\right)}$$

$\bar{\theta}_R$ assumed as -1.75 K day^{-1} (Betts and Albrecht, 1987).

From the values of Table 1, for isolated vis-a vis widespread category, we get

$$\bar{P}_{SLR} = 12.2 \text{ hPa day}^{-1} \quad \text{and}$$

$$\bar{P} = 12.2 - 27.8 = -15.6 \text{ hPa day}^{-1}$$

which is in agreement with the change in -56 hPa in 3.6 days , Betts and Albrecht (1987) have shown that the longer the air subsides the more negative P^* becomes. The minimum value of P^* at the top of the CBL therefore indicates that air has subsided the longest.

4.4.4 Internal CBL Structure

The vertical distribution of the thermodynamic parameters can be characterized by the mixing line (ML) and the location of SP on it. In the mixing line parameterisation for the CBL (Betts, 1985,1986), the slope of the mixing line is determined by mixing air near the surface with air above the CBL top and the distribution of SP within the CBL can be specified along this mixing line using an empirical parameter β defined as

$$\beta = \frac{\partial p_{SL}}{\partial p}$$

The β values in the subcloud (Sc), cloud (c) and in the overlying stable layers (I) computed for the four categories are given in Table 2. The SP distribution in subcloud layer is not on the ML but on the dry virtual adiabat (constant θ_v). In the subcloud layer $\beta_{SC} = 0.76$, on the average, which is higher as compared to 0.3 , suggested by Betts and Albrecht (1987). The higher side of β in the subcloud layer may be the typical characteristic feature of monsoon boundary layer. As $\beta = 0$ represents a well-mixed layer, β_C values here also suggest the subcloud layers are not well mixed. In cloud layers (β_C) and capping layers (β_I), the average values are 1.05 and 1.41 respectively. It also is seen that as the CBL top increases (which is associated with increasing rainfall activity), β_I decreases (i.e. the inversion layer decreases). .Denoting Γ as lapse rate computed from cloud base to cloud top and cloud base to CBL top, Γc and ΓI show increasing trend (from 4K to 5K) with increasing CBL tops (Table 2). The above results are comparable with those obtained from CBL study for the Pacific ocean.

5 Conclusions

The study of the structure of Convective Boundary Layer (CBL) over the Deccan Plateau region of India during two summer monsoon seasons using the approaches of Saturation Point (SP)and mixing line (ML) , as suggested by Betts (1982),have brought out the following interesting features.

On the average CBL top was at 650 hPa. The CBL heights during different weather conditions, determined by the rainfall activity in the region, were found to be between 700-600 hPa. The CBL heights thus obtained could be considered as the distance up to which the surface properties could be coupled thermodynamically in the vertical direction. The CBL tops in the four categories with increasing rainfall /monsoon activity were determined as 700, 650, 630 and 600 hPa, showing larger extent of CBL with deep rainfall activity. Based on Conserved variable diagrams (θ_e-q) which illustrate the role of radiation, precipitation and mixing processes in maintaining the CBL structure, during different weather conditions showed characteristic mixing line structures from the surface to the top of the CBL. The Isolated rainfall category was distinguished from other categories such as extension of CBL top to 700 hPa and appearance of SP at longer distances between 750-700 hPa due to the presence of strong stable layer. The mixing line slope has also gradually increased with increase in rainfall activity i.e. mixing line tried to attain stability as the rainfall activity increased from Isolated to Widespread rainfall category.

In general, the CBL structures, from surface to the top of the CBL, during different categories represented by a single mixing line showed uniform progression of thermodynamic structure with increasing rainfall. During active monsoon conditions the cloud layer was represented by constant subsaturation i.e. nearly constant P^* values,. while P^* showed strong negative gradient in the strong stable layer between 750-700 hPa during the break monsoon conditions.

The origin of the CBL top air was estimated by from the conservation of q. The q value at the CBL top in the Isolated rainfall category was 5.9 gm kg^{-1}. This value of q was observed at 600 hPa in the Widespread rainfall category. The CBL top air in the Widespread category appeared to subside from 600 hPa to 700 hPa with a rate of subsidence 28 hPa day^{-1}. The rates of subsidence of the CBL top air in the Isolated rainfall category and weak monsoon condition were found to be 28 hPa day^{-1} and 32 hPa day^{-1} respectively.

Acknowledgements

The author is thankful to the Director of the Institute for the facilities provided for this study. Shri T.A.Disale has helped in the preparation of the manuscript of this paper.

Table 1 : SP parameters for the CBL top for isolated / widespread rainfall categories and break/active monsoon

Rainfall category	P hPa	T_{SL} (°C)	P_{SL} (hPa)	θ (K)	q gm kg^{-1}	θ_e (K)	P^* (hPa)
(a)Isolated	700	-1.7	602	313.9	5.9	331.7	-98
(b)Widespread	600	-2.3	558	320.2	5.9	338.1	-42
(c)Break monsoon	700	-4.2	562	317.2	5.4	333.5	-139
(d)Active monsoon	520	-4.8	500	327.2	5.4	343.6	-20

difference	Δp	ΔT_{SL}	ΔP_{SL}	$\Delta\theta$	Δq	$\Delta\theta_e$	ΔP^*	Δt in days	ω hPa per day
(a)-(b)	100	-0.6	44	-6.3	0.0	-6.4	-56	3.6	27.8
(c)-(d)	180	-0.6	62	-10.0	0.0	-10.1	-119	5.7	31.5

Table 2 : CBL parameters

Rainfall category	β_{SC} sub Cloud	β_C Cloud	β_i Inversion layer	CBL top (hPa)	Γ_C (K/100 hPa)	Γ_I (K/100 hPa)
Isolated	0.70	1.10	1.94	700	-4.13	-3.98
Scattered	0.74	1.04	1.38	650	-4.71	-4.54
Fairly Widespread	0.73	1.00	1.22	630	-4.45	-4.91
Widespread	0.86	1.04	1.10	600	-4.76	-5.24
Mean	0.76	1.05	1.41			

REFERENCES

Betts, A.K., 1982 : Saturation point analysis of moist convective overturning. *J. Atmos. Sci.,* **39**, 1484-1505.

Betts, A.K., 1986 : A new convective adjustment scheme. Part I : Observational and theoretical basis. *Quart. J. Roy. Meteor. Soc.,* **112**, 677-691.

Betts, A.K., and M.J. Miller, 1986 : A new convective adjustment scheme. Part II : Single column tests using GATE-Wave, BOMEX, ATEX and Arctic airmass datasets. *Quart. J. Roy. Meteor. Soc.,* **112,** 693-709.

Betts, A.K., and B.A. Albrecht, 1987 : Conserved variable analysis of the convective boundary layer thermodynamic structure over the tropical oceans. *J. Atmos. Sci.,* **44**, 83-99.

Boers, R. and A.K. Betts, 1988 : Saturation point structure of marine stratocumulus clouds. *J. Atmos. Sci.,* **45**, 1156-1175.

Holt, T. and S. Sethuraman, 1986: Observations of the mean and turbulence structure of the marine boundary layer over the Bay of Bengal during MONEX-79. *Mon.Wea.Rev.*, **114**, 2176-2190.

Parasnis, S.S., 1991 : Wind characteristics in the lowest 340 m of the atmospheric boundary layer. *Boundary-Layer Meteorol.*, **54**, 277-285.

Selvam, A.M., S.S. Parasnis, A.S. Ramachandra Murty and Bh.V. Ramana Murty, 1982 : Evidence for cloud top entrainment in the summer monsoon warm stratocumulus clouds. *Proc. Conf. on Cloud Physics,* Chicago, USA, 151-154.

Sikka, D.R., 1978 : Some aspects of life history, structure and movement of monsoon depressions. In *Monsoon Dynamics* (edited by T.N. Krishnamurty), pp. 1501-1529, Birkhauser, Basel, Switzerland.

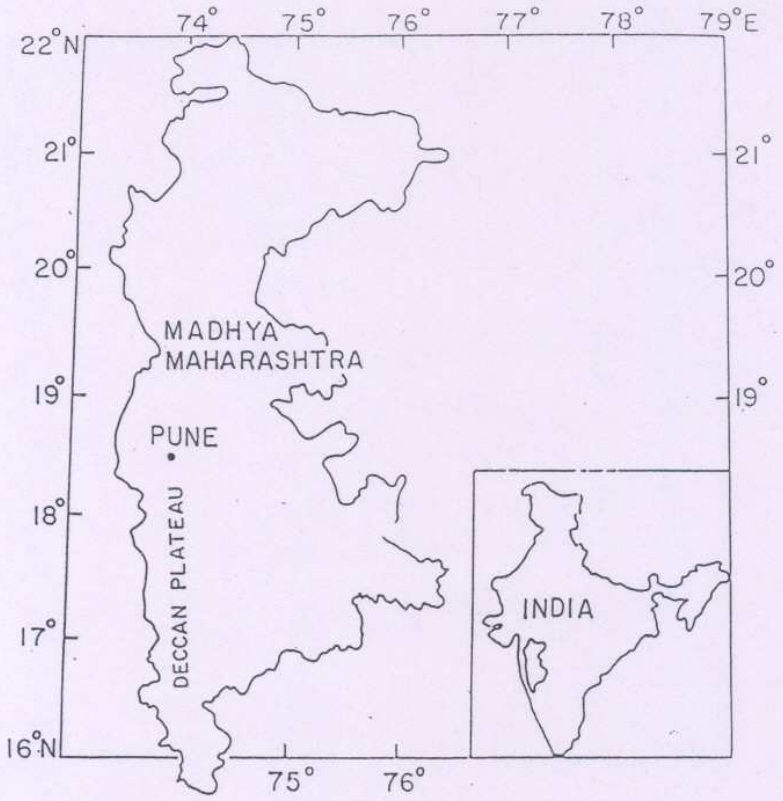

Figure 1 : Map showing the locations of Pune,Deccan Plateau and Madhya Maharashtra,India

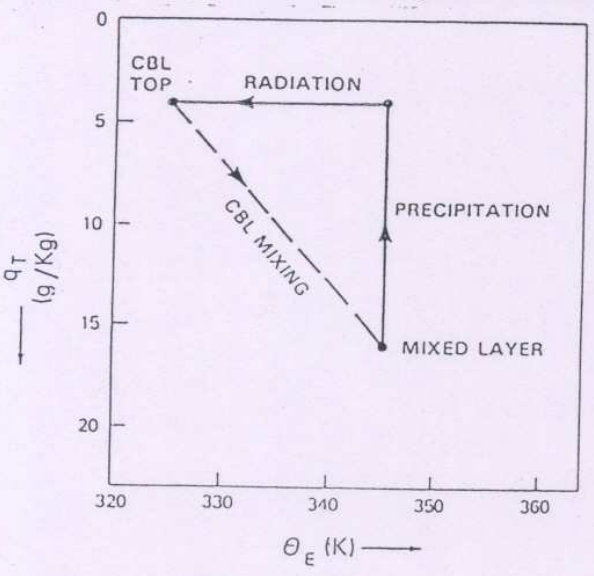

Figure 2 : Conserved variable diagram showing different atmospheric processes (Betts and Albrecht,1987)

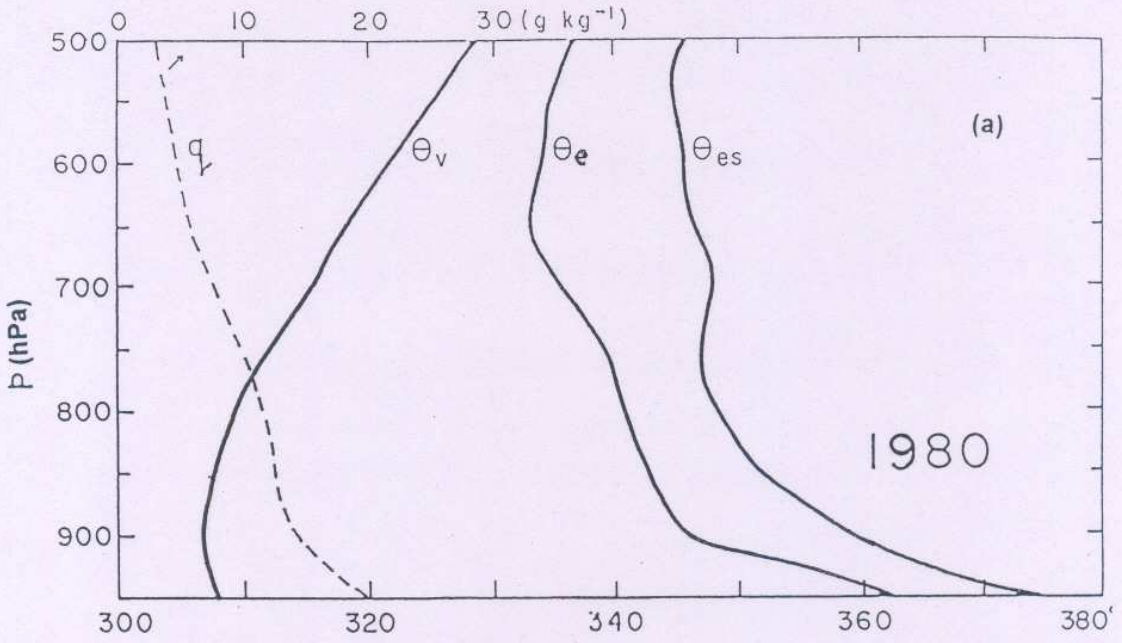

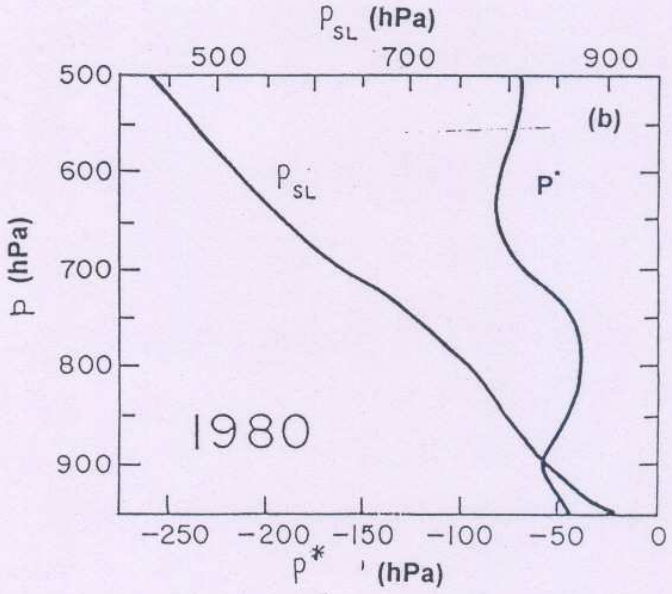

Figure 3 (a) : Vertical profiles of q, θv, θe, θes for the summer monsooon of 1980

Figure 3(b) : Plots of P and P^{*} for 1980

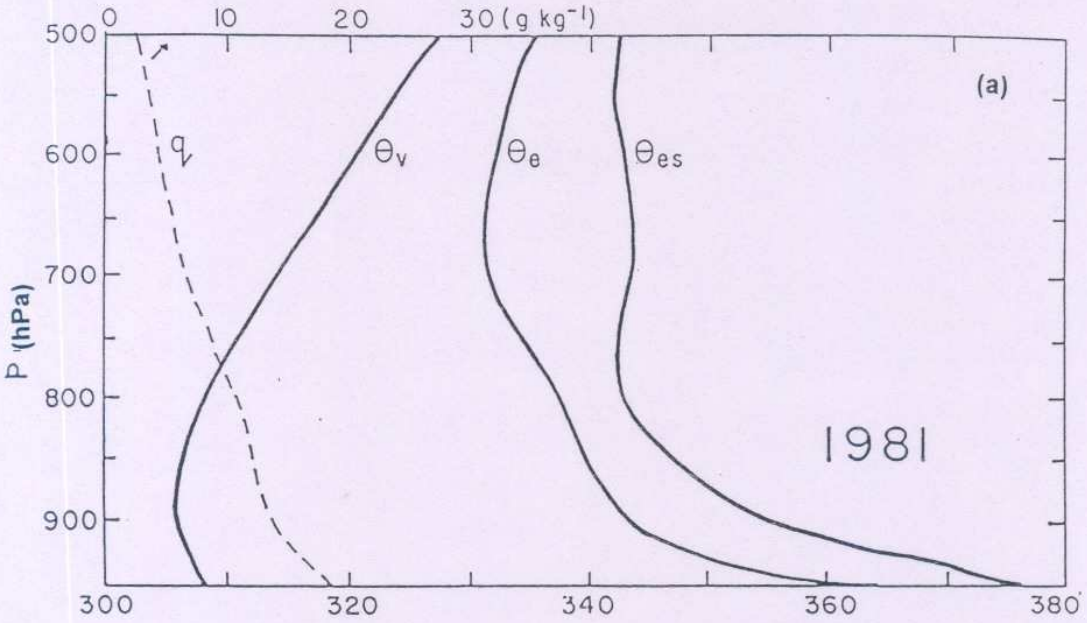

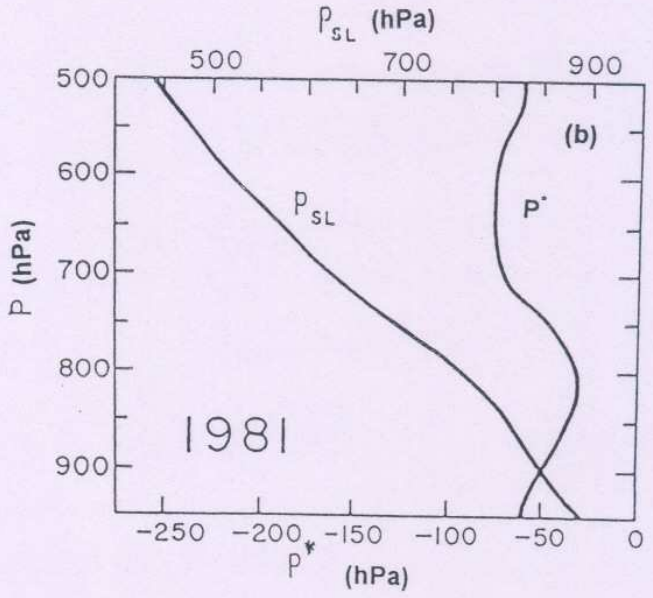

Figure 4 (a) : Same as Figure 3(a) but for 1981

(b) : Same as Figure 3(b) but for 1981

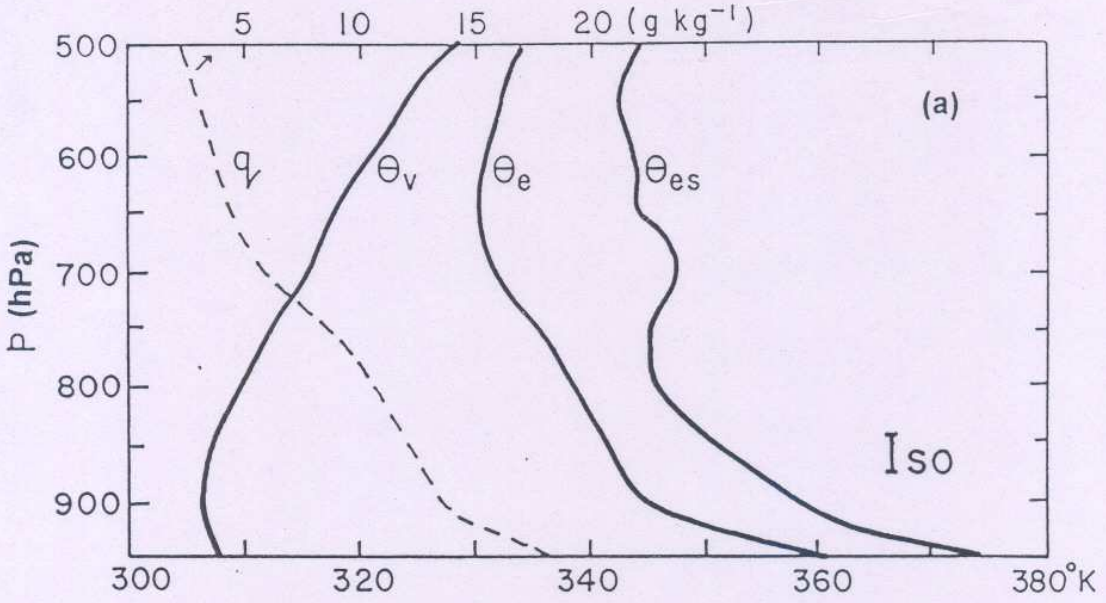

Figure 5 (a) : Vertical profiles of q, θv, θe, θes under isolated rainfall category

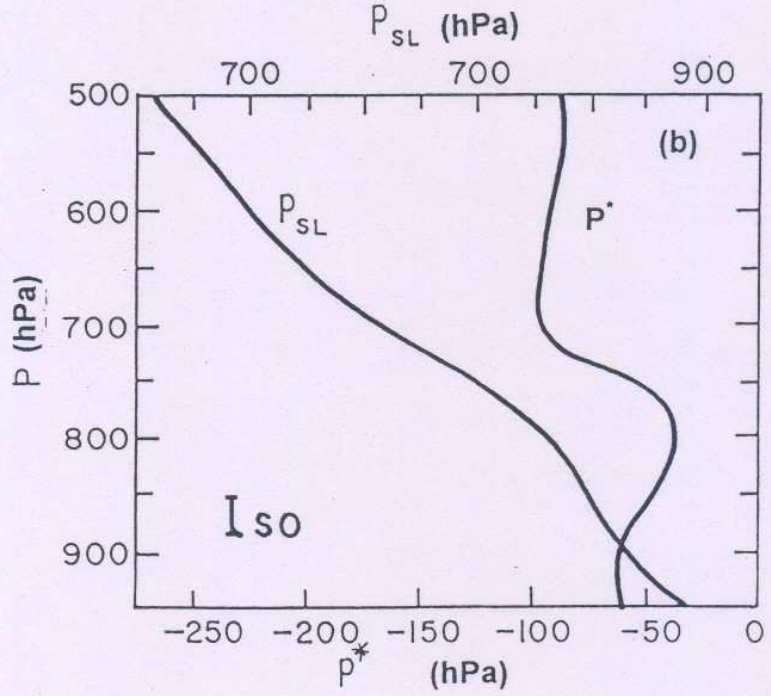

Figure 5 (b) : Plots of P and P* under isolated rainfall category (Iso)

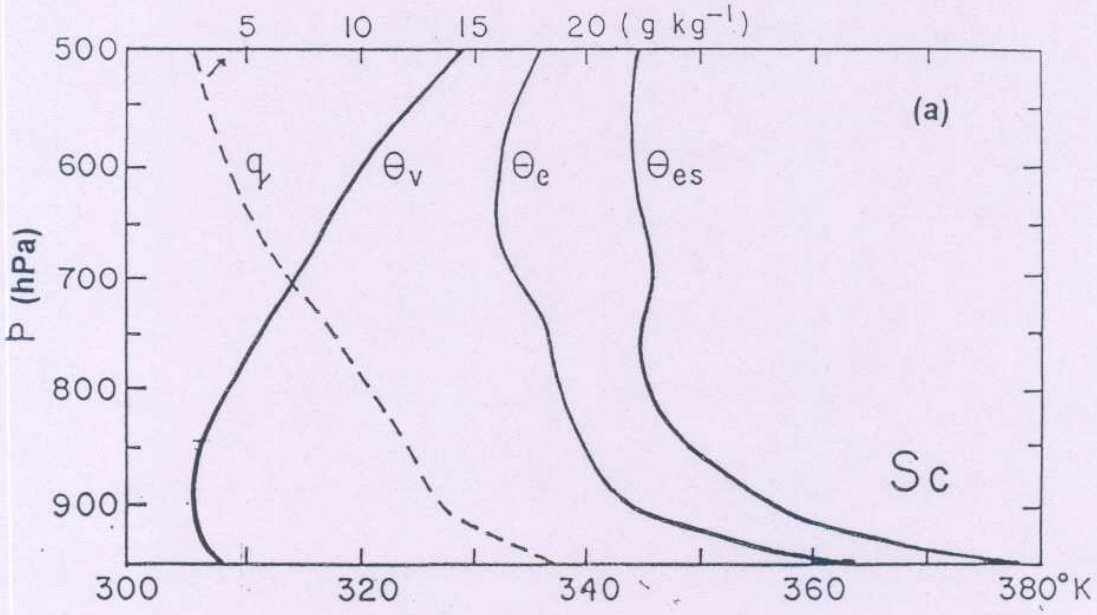

Figure 6 (a) : Vertical profiles of q, θv, θe, θes under scattered rainfall category

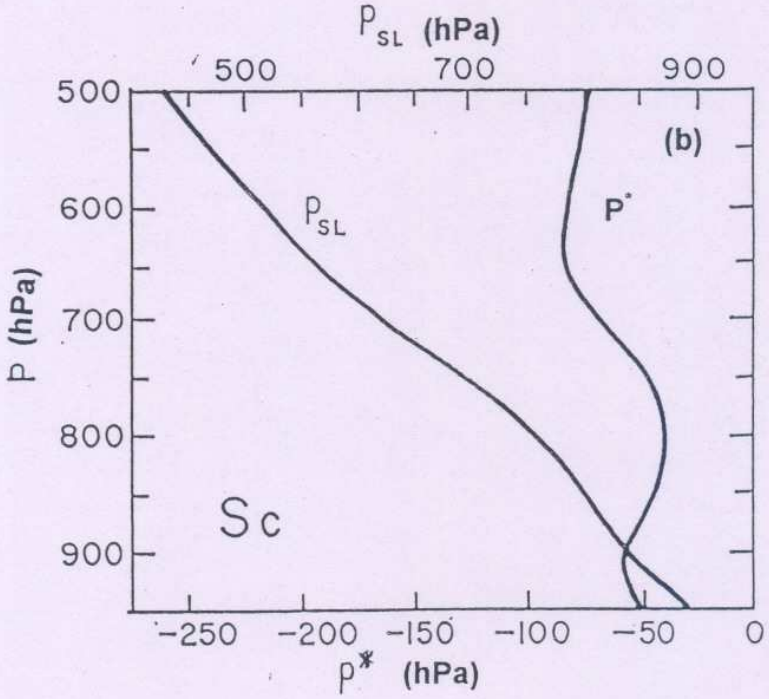

Figure 6 (b) : Plots of P and P* under scattered rainfall category (Sc)

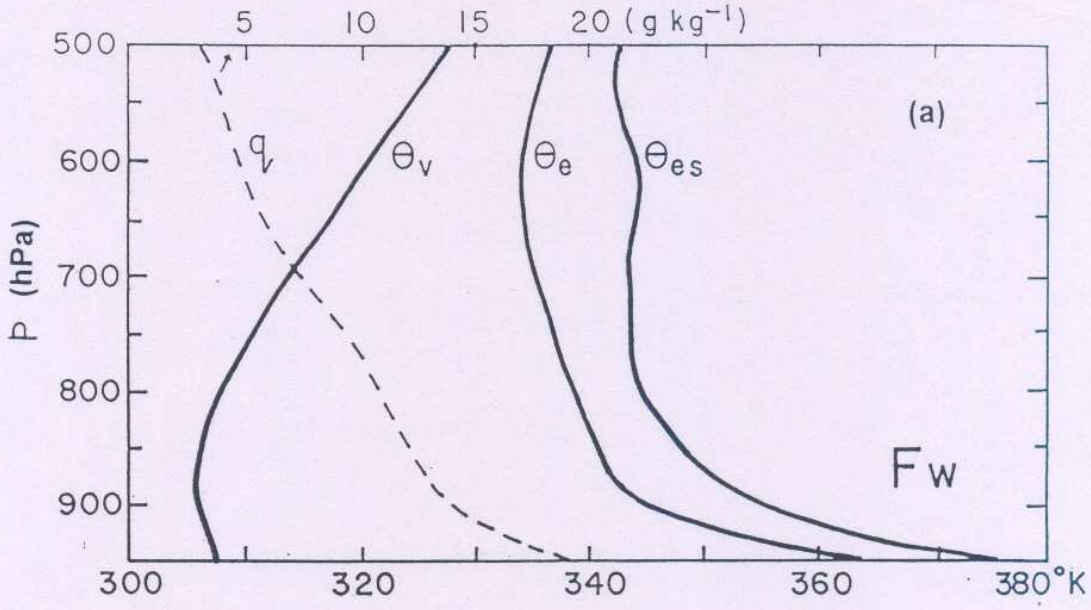

Figure 7 (a) : Vertical profiles of q, θv, θe, θes under fairly widespread rainfall category

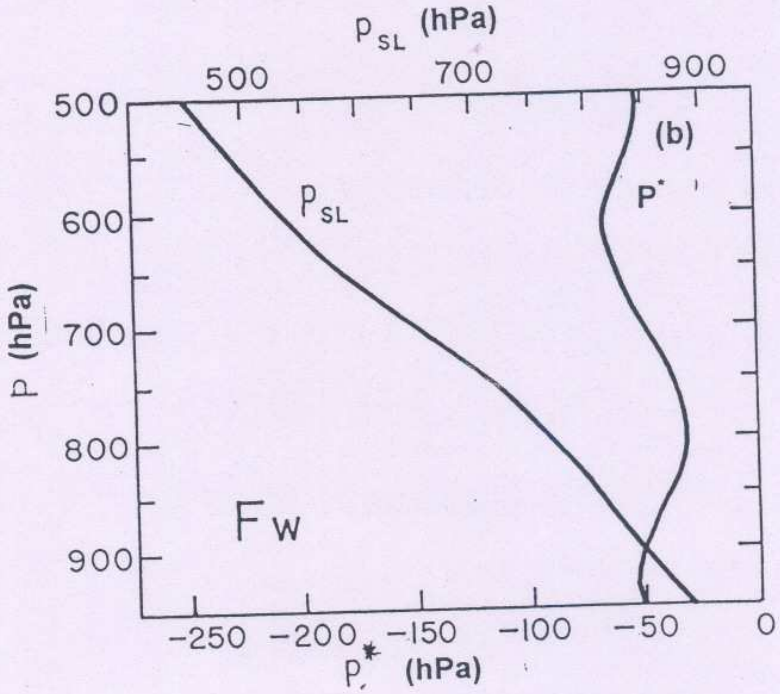

Figure 7 (b) : Plots of P_{SL} and P^* under fairly widespread rainfall category (FW)

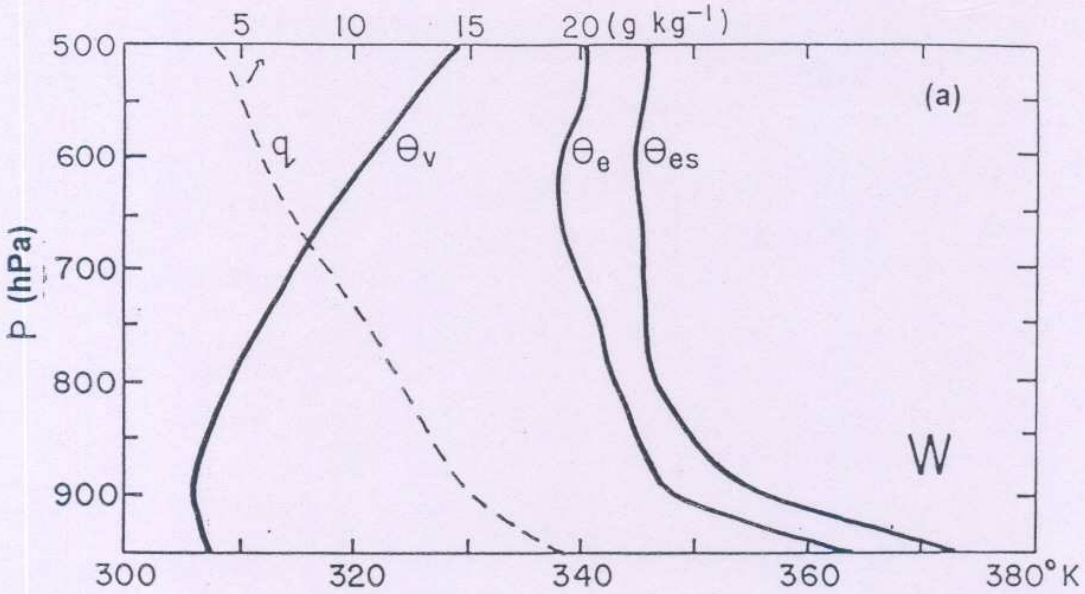

Figure 8 (a) : Vertical profiles of q, θv, θe, θes under widespread rainfall category

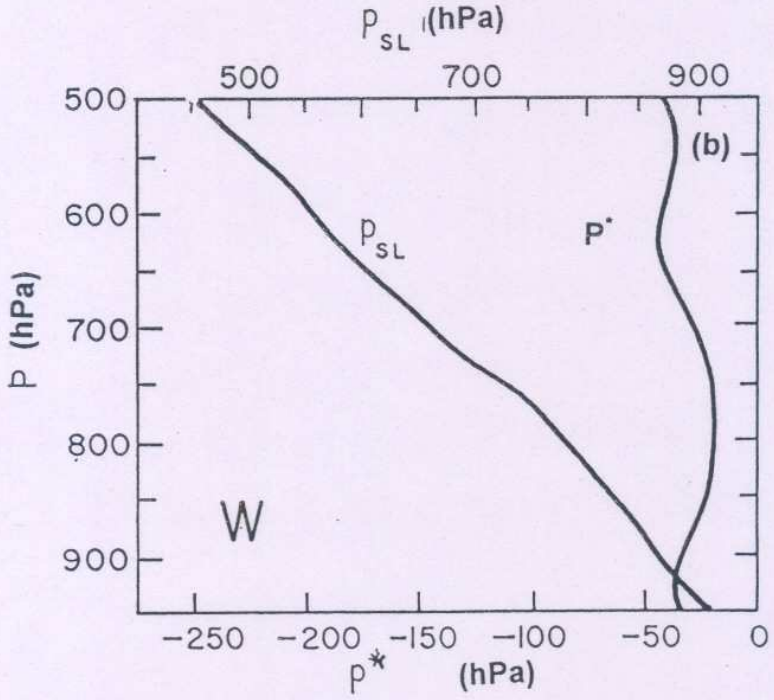

Figure 8 (b) : Plots of P_{SL} and P^* under widespread rainfall category (W)

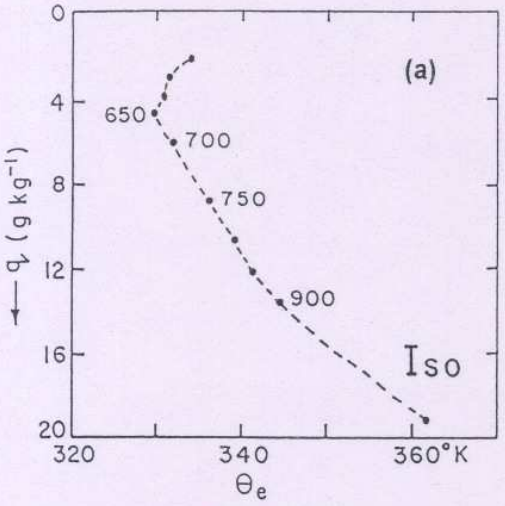

Figure 9 (a) :

Conserved variable plot of θe against q under isolated rainfall category

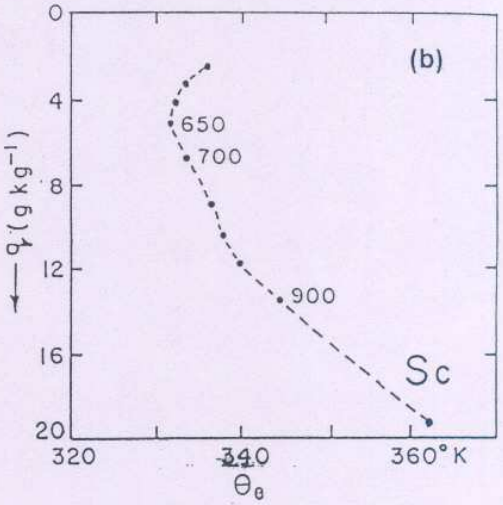

Figure 9 (b) :

Same as Figure 9 (a) but under scattered rainfall category

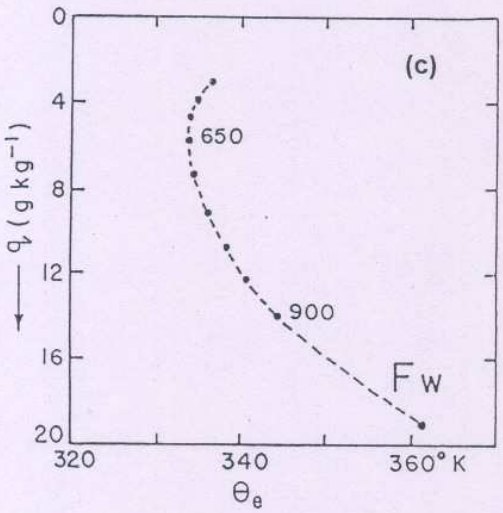

Figure 9 (c) :

Same as Figure 9 (a) but under fairly widespread rainfall category

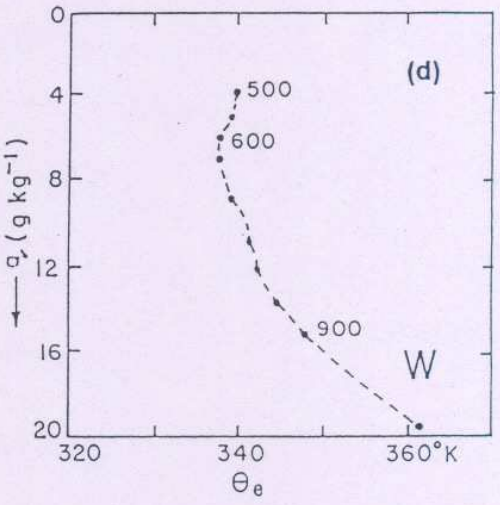

Figure 9 (d) :

Same as Figure 9 (a) but under widespread rainfall category

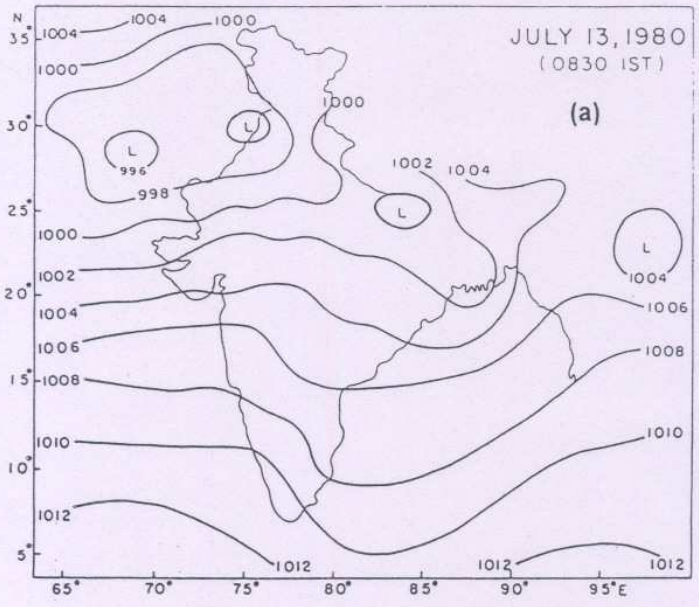

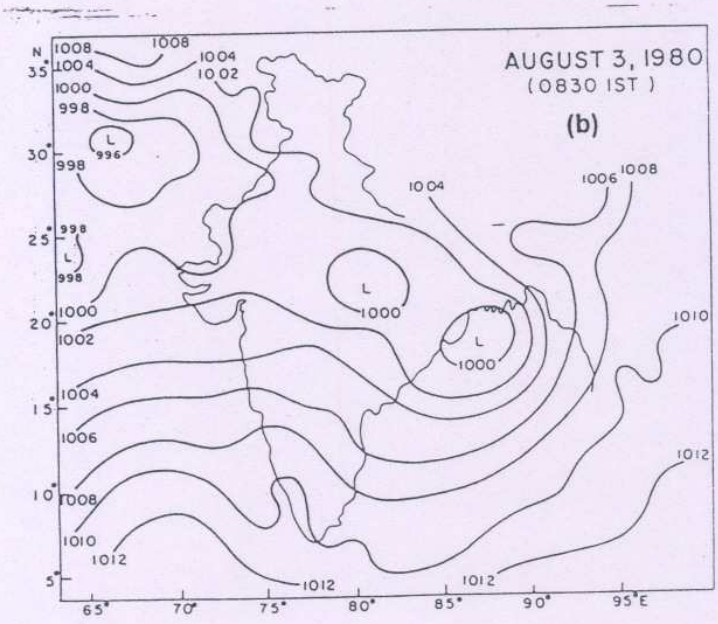

Figure 10 : MSL pressure chart on (a) July 13,1980 indicating 'break monsoon' and (b)Aug.3,1980indicating 'active monsoon'

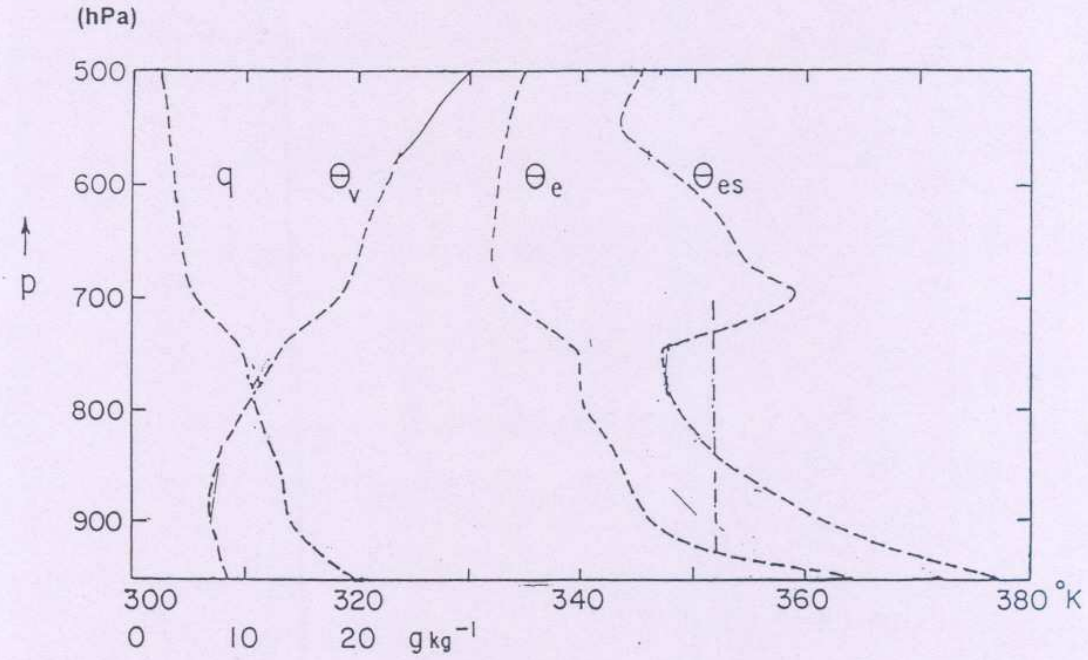

Figure 11 (a) : Vertical profiles of q, θv, θe, θes during 'break monsoon' period (12-17 July,1980)

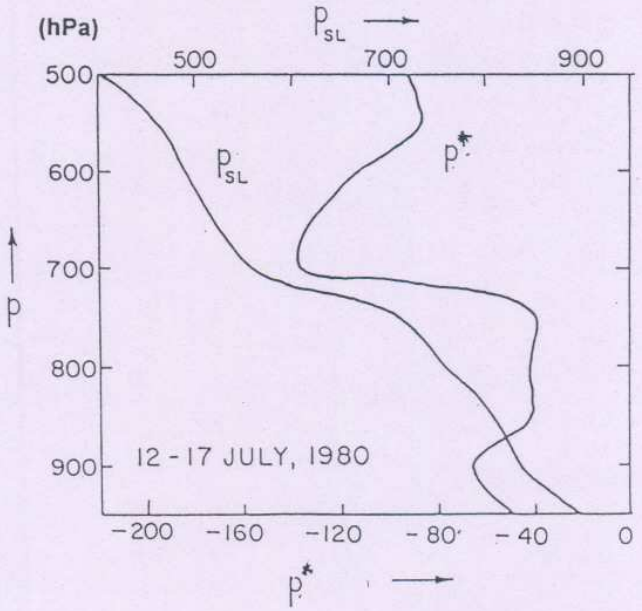

Figure 11 (b) : Plots of P_{SL} and P^* during ' break monsoon' period (12-17 July,1980)

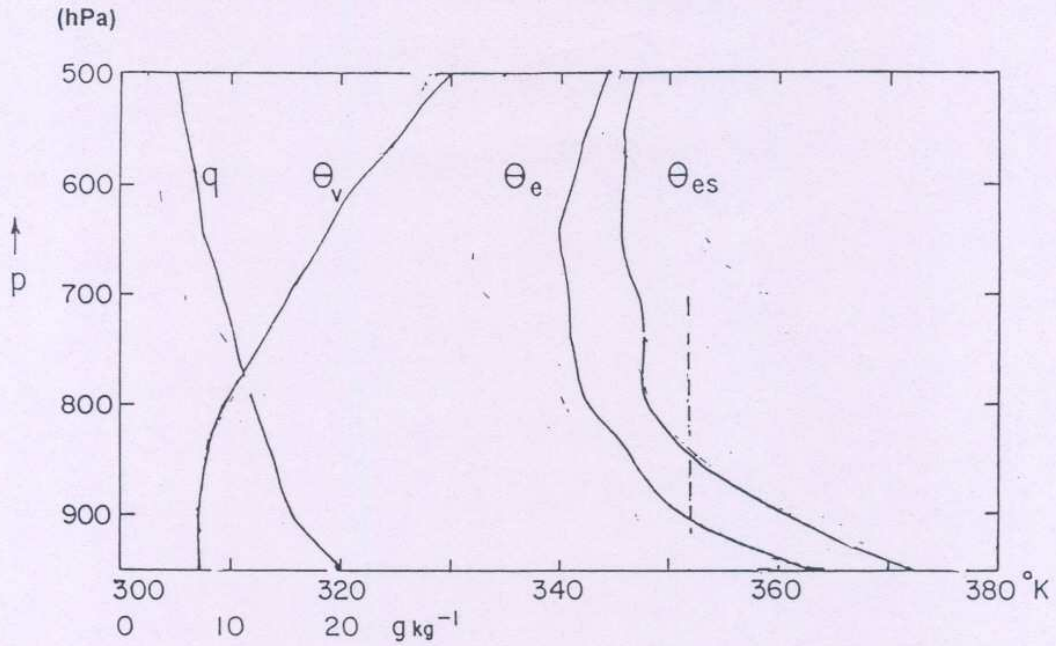

Figure 12 (a) : Vertical profiles of q, θv, θe, θes during ' active monsoon' period (1-5 Aug.1980)

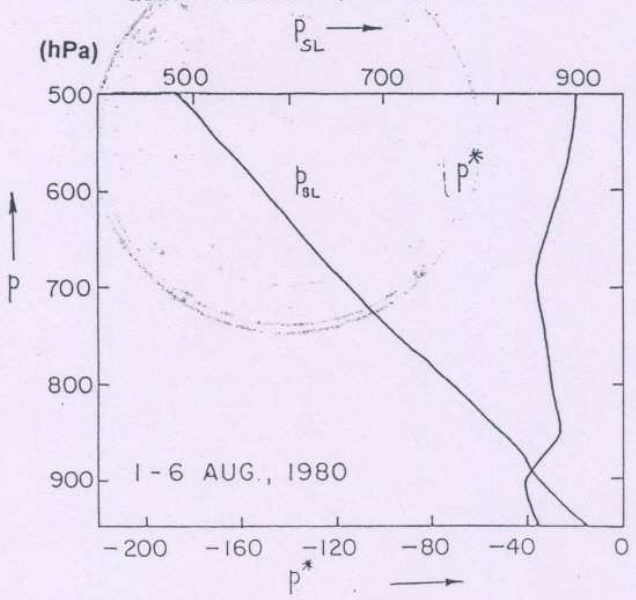

Figure 12 (b) : Plots of P_{SL} and P^* during ' active monsoon ' period (1-5 Aug,1980)